Title: **Investigating Neural Connectivity in Psychosis: A Dynamic Causal Modeling Approach with EEG Biomarkers and Biotype-Specific Analyses**

Course: MRes Brain Sciences

Candidate Number: **JLPF9**

Word count: 5560

Declaration

I, **JLPF9**, confirm that the work presented in this thesis is my own. Where information has been derived from other sources, I confirm that this has been indicated in the thesis.

The MATLAB scripts and DCM model running DCM analysis and simulation was provided by Dr Rick Adams and Julia Rodriguez Sanchez

.

PERSONAL ACKNOWLEDGEMENT

I would like to sincerely thank my parents for their unwavering support and encouragement throughout this journey. Their belief in me has been a constant source of inspiration. I am also deeply grateful to my girlfriend, Yijin, for helping me navigate the challenges of this project. Her understanding and encouragement have been invaluable. To my family, my partner, and my friend, thank you for being a pillar of strength and support, and for playing a vital role in my success of this project.

Investigating Neural Connectivity in Psychosis: A Dynamic Causal Modeling Approach with EEG Biomarkers and Biotype-Specific Analyses

JLPF9, Division of Psychiatry, University College London

Corresponding author: JLPF9

JLPF9, anonymouse.ucl.ac.uk

Short title: Neural Connectivity in Psychosis: A DCM and EEG Study

Key words:

Schizophrenia, Dynamic Causal Modeling, Electroencephalography, Brain Connectivity, biotype, excitation/inhibition balance, psychosis

Abstract

Background: Disruptions in excitation/inhibition (E/I) balance are key to the neurophysiological changes observed in psychosis. Recent studies have identified distinct biotypes within psychosis. This study explores the unique connectivity pattern of each biotype to examines how E/I imbalances manifest across biotypes using Electroencephalography (EEG) analysis and dynamic causal modelling (DCM).

Methods: Resting-state EEG data from the B-SNIP dataset (n=2450) were analyzed using power spectral density (PSD) analysis, sensor-level topographical mapping, and source reconstruction. Initially, DCMs was employed, but due to model fit issues, simulations with conducted to reproduce the group effects in biotypes.

Results: The PSD analysis revealed increased theta and gamma power and decreased beta power in patients compared to healthy controls. Topographical mapping indicated significant differences in the theta and gamma bands, particularly in frontal, parietal, and occipital regions. By incorporating priors, source reconstruction confirmed the region of interest for DCM, however the model does not fit. Subsequent simulations highlighted potential neural connections responsible for the group differences, suggesting that alterations in intrinsic connectivity, particularly in inhibitory interneurons and pyramidal cells, may drive the neurophysiological distinctions among the biotypes.

Conclusions: While this study provides some evidence into the connectivity differences in neural circuits in relation to biotype-specific connectivity patterns, the results are limited and requires further investigation. Although the findings offer partial support for the hypothesis that E/I imbalance underlies the distinct biotypes, additional research is needed to validate these patterns and further explore their neurobiological significance.

Introduction

Psychotic symptoms are disruptions of reality experiencing and are seen in severe mental illnesses including schizophrenia, schizoaffective disorder and bipolar disorder with psychotic features. These conditions are characterised by the presence of severe symptoms such as disruptions in perception, cognition, and behavior which include hallucination and delusions. The conventional approach for diagnosis mainly based on their symptoms, however, did not account for the neurobiological heterogeneity of the disorders. Because the disorders might share common symptoms, traditional diagnosis can lead to challenges and poor treatment outcomes[1]. A more evidence-based classification of the disorder that is based on biological findings has been required[2].

Biomarkers afford a potentially powerful approach to enhancing the identification and management of psychiatric disorders by quantifying the biological substrates of these conditions. Improvement in the neuroimaging and electrophysiological tools such as EEG and fMRI has enhanced the creation of biomarkers for psychosis. These biomarkers can help to move beyond the current global approach to the neural basis of psychotic disorders and thus aid in the formation of more targeted treatment plans[3].

The theories of E/I imbalance have recently received attention in providing an account for the neural basis of schizophrenia. This imbalance is defined by an instability of the balance between excitation and inhibition in the brain which is believed to explain the altered neuronal connectivity found in psychosis[4]. The use of DCM to EEG data in this framework enables examination of these E/I dysregulations at the circuit level, which may help elucidate how such disruptions may manifest in symptoms or neurophysiological endophenotypes of psychosis[5]

A number of research has indicated that biomarker-based approaches might improve the management of psychosis. For instance, Adams et al.[4] showed that a decrease in the synaptic gain in pyramidal cells is a fundamental feature of schizophrenia and has a strong effect on EEG and fMRI indices. In addition, Clementz et al.[6] has classified the psychosis into three biotypes through a series of biomarkers that include the neuropsychological tests, stop signal tasks, saccadic control and auditory stimulation paradigms. These measures were statistically subsided into nine composite variables that explained neurobiological heterogeneity of psychosis. Three neurobiologically derived subtypes were then identified through multivariate taximetrics analyses and externally validated by social functioning, structural MRI, and familial biomarkers. This biomarker-based approach to subset these patients based on their neurobiological characteristics was far more reasonable than relying on the current diagnostic categories.

With these findings in mind, this study aims at comparing brain connectivity

between healthy subjects and patients with psychosis as well as the three psychosis biotypes. By using various methodological approaches such as spectral analysis, sensor-level topographical mapping, source reconstruction and DCMs, this study seeks to explain the neurobiological basis of these conditions. The current study seeks to establish the differences in connectivity patterns between the healthy controls and patients with psychosis with the view of determining how these differences can be used to explain the alterations in brain circuits, specifically about the E/I imbalance, that are associated with psychosis.

Methods and Materials

Participants

Resting state EEG data from B-SNIP study

The data used in this study were collected in the Bipolar-Schizophrenia Network on Intermediate Phenotypes (B-SNIP) study (n=2450) which offers neuroimaging, electrophysiological, and clinical information for patients with schizophrenia, schizoaffective and bipolar disorder with psychotic features. The participants are recruited from six sites in the US with similar recruitment criteria. This dataset employed in this study consists of resting state EEG data obtained from patients with schizophrenia (n=397), schizoaffective disorder (n=223), and bipolar disorder with psychosis (n=312), their first-degree relatives (n=408, 262, 358), and healthy subjects (n=455). The EEG data was acquired under both eyes-open (EO) and eyes-closed (EC) condition.

For this study, the participants have been analysed based upon their demographic factors and thus have been grouped into three main categories based on clinical data. The first group is Healthy Control (HC) which include participants who have no history of psychosis in themselves or their first-degree relatives, against whom all the other groups are compared. The second group, Probands, is composed of clients who have been medically confirmed to have one of the major psychotic disorders, which are schizophrenia, schizoaffective disorder or bipolar disorder with psychotic features. The third group includes Relatives of these probands—first degree relatives of the patients who may not themselves have a psychotic disorder but have a higher risk because of their genetic link.

Biotype Classification

Besides the initial B-SNIP categorization, this study also employs the new classification system by Clementz et al.[6] that groups patients based on biological factors, not only on the basis of symptoms. This data-driven approach defines three different biotypes within psychosis spectrum with the goal of better characterizing the

heterogeneity of the disorder by looking at the brain function.

Biotype 1 is characterized by severe neurobiological impairments such as cognitive deficit and disrupted connectivity in the brain. These individuals generally have the most severe symptoms as well as the most severe level of brain impairment. Biotype 2 involves individuals with moderately severe neurobiological alterations with definite dysconnectivity of the brain and relatively milder cognitive deficits as compared to Biotype 1. Last but not least, Biotype 3 represents subjects with fairly normal neurobiology, as well as the cognitive performance and brain connectivity that are comparable to those of HC.

Data Preprocessing

EEG data were recorded using high density systems, with 64 or 62 electrodes used in the collection process. The data were recorded at 1250 Hz. The EEG data which were to be analysed were first prepared in several significant preprocessing steps with the help of SPM12. The raw EEG data were first transformed into SPM format which is the format that SPM 12 can work with. The EEG sensor locations were then reset to the standard positions. The montage of the EEG channels was then transformed so that it conforms to the standard electrode placement scheme. The raw data was then down-sampled to 250Hz for the purpose of reducing file size and computational complexity without losing important frequency content. Last of all, the EEG signals were re-referenced where the signals were recalculated relative to a common reference to reduce noise and enhance the quality of the signals.

The preprocessing steps were performed with the support of MATLAB R2023b and SPM12 (v7771) and some additional custom developed scripts. The first step involved importing of the EEG data and the grouping information of the participants in the study from an Excel file. The participants were first divided into groups depending on their clinical diagnosis. Then, the power spectral density (PSD) of the EEG signals was calculated with the Welch method which is one of the most popular techniques that estimate the power of the signal within the different frequency bands by subdividing the signal into overlapping segments, applying window function and averaging periodograms of these segments[7]. The PSD was calculated over the frequency range of 4 to 50 Hz paying special attention to the theta (4-7 Hz), alpha (8-14 Hz), beta (15-30 Hz) and gamma (31-50 Hz) bands that are linked with different cognitive and neural functions[8]. The EEG data matrix of each subject contains two dimensions: channel and frequency point, where the trials are averaged when applying the Welch function. To increase the reliability of the analysis, the outlier removal was done through the use of 'filloutliers' function which is based on quartiles and a factor of 3[9]. This approach detects outliers by comparing the values for each frequency-channel point of the whole

population in order to exclude the impact of these values on the results. The matrix was then averaged over the channels to compute the PSD for each subject and over subject for the group mean power. In averaging, all the data points which were eliminated from the data are completely neglected.

Power Spectrum Analysis and Visualization

After obtaining the PSD in the various frequency bands, the next step was to plot the data in order to compare the spectral power between the groups. First of all, line plots were created to display power spectra for each group: Healthy Controls, Patients, Relatives, and Biotypes under EO and EC conditions to get a better understanding of how power values were distributed across frequency bands within each group.

Boxplots were also plotted with scattered data points demonstrating the distribution of power within each frequency band. These box plots provided a more comprehensive way of comparing the two groups as it also showed the mean, median, range within the middle 50% and the outliers if any. By using ANOVA and Tukey's HSD, the boxplots highlighted the significant differences between groups in each of the frequency bands.

Sensor-Level Analysis

Topographic analysis was used to display the spatial distribution of group effects in the scalp EEG activity. The analysis was conducted using MATLAB and FieldTrip functions[10]. The data was pre-processed via steps such as defining channel labels, electrode positions, and the frequency range and arranged in a way that was compatible with FieldTrip so that all the information that would be required for surface mapping was well portrayed. n this step, the subject EEG data matrices was not averaged over the channel, but the averaging was over the frequency points for each of the frequency bands. Topographical maps were then generated for each group and frequency band using the ft_topoplotTFR function[10]. Statistical comparisons between groups were done using t-tests, which assessed whether the differences in spectral power between groups were statistically significant. These significant differences were then visualized on topographical maps that used the data by subtracting averaged HC data by the patients' groups, highlighting the channels where the group differences were most pronounced.

Source Reconstruction

At first, beamforming technique was applied but later on MSP was used because beamforming gave more noisy output. MSP was especially preferred for its efficient incorporation of prior information that had coordinates determined by prior studies to obtain correct spatial localization of neural generators from the EEG data[11].

Two sets of regions of interest were suggested from the previous studies for the use of MSP. Symmonds et al[12]. identified the regions within the DMN as the prior set of regions for MSP. This network, which is active during resting states and related to higher-order cognitive functions, comprises primary source seeds in the left and right parietal cortices at MNI coordinates (-29, -68, 49) and (29, -68, 49), as well as the left and right prefrontal cortices at MNI coordinates (-33, 45, 28) and (33, 45, 28).

Because of the potential relationship between group differences in EEG signals and the visual cortex in the occipital region with regards to the Gamma band, another set of priors was used, as proposed by Grent-'t-Jong et al.[13]. The selected regions for this analysis are the left and right primary visual cortex, with MNI coordinates at [-11 -81 7] and [11 -78 9]. However, the specific coordinates were not directly provided in the original article of the study, they were determined using the BioImage Suite tool, as outlined by Lacadie et al.[14].

Dynamic Causal Modeling

The first neuronal model used (spm_fx_cmc_ei_v1) was an updated version of the Canonical Microcircuit (CMC) model, including four distinct neuronal populations: spiny stellate cells, superficial pyramidal cells, inhibitory interneurons, and deep pyramidal cells (Figure 1). Comparing with the default CMC model, this updated model included changes such as the removal of the spiny stellate to superficial pyramidal (sp->ss) connection, and the addition of superficial pyramidal to deep pyramidal (sp->dp) and superficial pyramidal to inhibitory interneuron (sp->ii) connections. It was further edited to estimate only 5 of the connections, including sp-sp, ii-ii, sp-ii, ii-sp and ss-sp

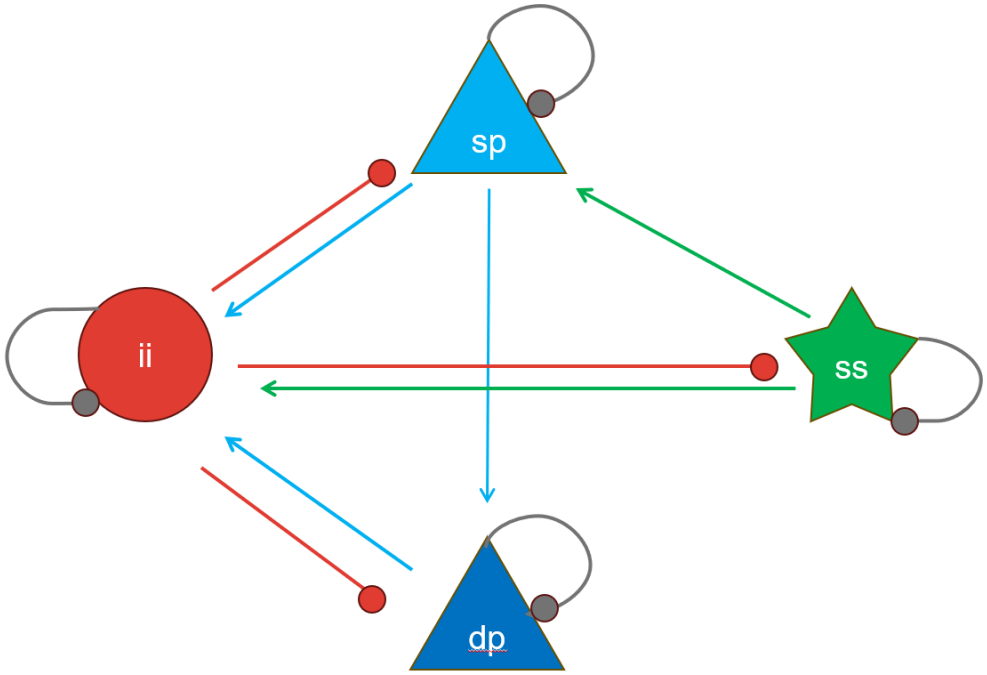

Figure 1: Figure illustration of the spm_fx_cmc_ei_v1 model with four cell populations and the 12 intrinsic connections.

Initially, The DCMs were performed with focus on Theta and Gamma bands respectively as well as full frequency band to attempt to fit both individual subjects from the HC group and the group mean data. However, all the DCMs didn't fit the data at all. The reason was considered to be the restriction of this model that it only estimates 5 of the connections. To try to solve the problem, another model (spm_fx_cmc_2017_constG) was employed. This model is the fundamental version of the spm_fx_cmc_ei_v1. The have the same cell populations and connectivity structure. Instead of focusing on only 5 connections, spm_fx_cmc_2017_constG has the ability to focus on the estimation of all 12 connections. When actually using this model in DCMs, it still did not fit the real EEG data. In this case, the focus was turned from applying DCM to simulation. The simulation was then achieved by examining if any priors applied to the model could replicate a general EEG pattern and then the differences patterns observed in the biotype's spectra. The first step of the simulation is to generate simulated power spectra that has the same main shape of real spectrum, for example the alpha peak. This was achieved by adding priors to the model parameters that are not the intrinsic connections, such as the synaptic time constants and the slope of the neuronal activation function. The next step can then be a focus on exploring the intrinsic connectivity parameters. Each of these intrinsic connections was altered by 30% to examine how their changes could reproduce the observed differences in real spectra between healthy controls and the biotypes of schizophrenia. This step was designed to identify which specific neural interactions might be the cause of distinct EEG patterns associated with the biotypes.

Results

Sample Data Inclusion and Exclusion

The EEG data were organized into two conditions: Eyes Open and Eyes Closed and were analyzed both in combination and separately. The participants were categorized using two distinct classification methods as mentioned in the methods section. The first classification was based on clinical information, and the participants are divided into groups of Healthy Controls (HC), Probands with Schizophrenia, Probands with Psychotic Bipolar Disorder, Probands with Schizoaffective Disorder, and their respective relatives. For the purposes of this study, these groups were consolidated into three primary categories in which the all the psychotic subjects are combined into a patient's group. Thus, the three groups are Healthy Controls (n = 143 for EO; n = 93 for EC), Patients (n = 276 for EO; n = 208 for EC), and Relatives (n = 304 for EO; n = 234 for EC). The chi-square goodness of fit test was applied and the number of subjects in EO is significantly larger than that in EC conditions, with EO having significantly more samples than EC ($\chi^2 = 28.10$, $p < 0.001$).

The second classification method relied on biomarker data to categorize participants into Healthy Controls and three distinct Biotypes. In this classification, Healthy Controls (n = 143 for EO; n = 93 for EC) were compared against Biotype 1 (n = 91 for EO; n = 76 for EC), Biotype 2 (n = 75 for EO; n = 59 for EC), and Biotype 3 (n = 81 for EO; n = 50 for EC), enabling a more detailed examination of the differences within the patient population. Without the Relatives group, EO still have significantly more sample than EC ($\chi^2 = 18.78$, $p < 0.001$).

During the initial data processing, each EEG file was matched with subject IDs from the classification tables, ensuring accurate group assignments. The data were then meticulously grouped according to both clinical and biomarker-based classifications. For the Power Spectrum Analysis and Sensor-Level Analysis, outliers were identified at the channel and frequency point levels—outlier values were replaced with NaN and excluded from further calculations. For the Source Reconstruction and DCM stages, channels with outlier values were marked as bad channels, following the requirements for processing SPM meeg data. This approach led to the exclusion of certain subjects from Source Reconstruction and DCM analyses. Specifically, 27 subjects (12 Healthy Controls and 15 Patients) were excluded because all of their channels were marked as bad channels, making their data unusable for these analyses.

Power Spectrum Analysis

The power spectrum analysis provides an overview of the frequency distribution

of EEG signals across various participant groups, highlighting differences between healthy controls, patients, and relatives, as well as between healthy controls and biotypes. The analysis includes a combined eyes conditions as well as EC/EC respectively.

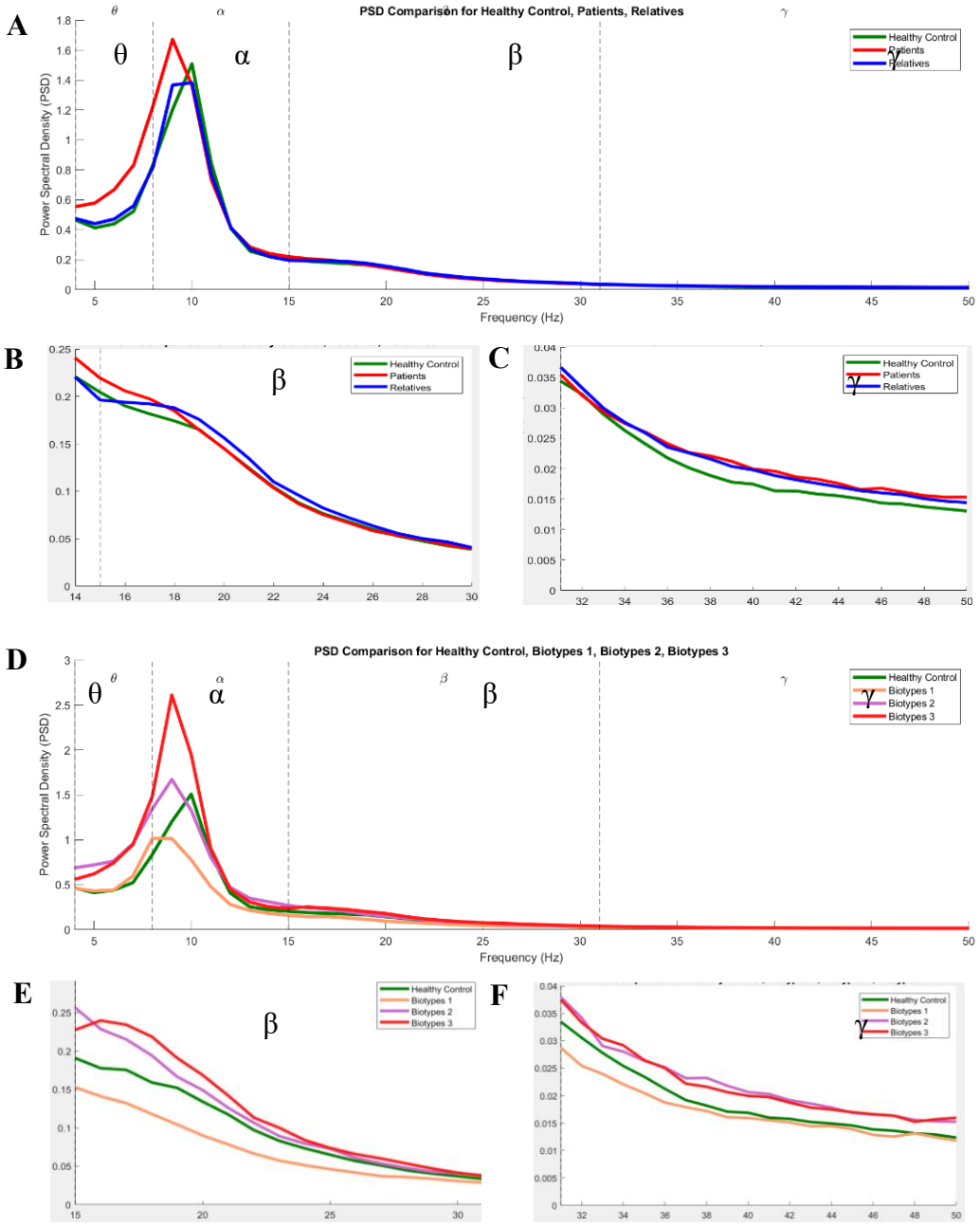

Figure 2: Power Spectral Density (PSD) comparison between groups with both EO and EC conditions with Beta and Gamma band zoomed in for clarity. (A), (B), and (C) PSD comparison for Healthy Controls (green), Patients (red), and Relatives (blud). fig.2B and C are enlarged sections of beta- and gamma-band respectively. **(D), (E), and (F)** PSD comparison for Healthy Controls (green) and Biotypes 1 (orange), 2 (purple), and 3 (red). Fig.2E and F are enlarged sections of beta- and gamma-band respectively.

With the combined conditions, as shown in figure 2, the power spectra across all groups show a consistent dominant peak in the Alpha band (8-12 Hz) and notable activity in the rest three bands. Patients tend to exhibit increased Theta, Alpha and Gamma power compared to HC. Relatives often show intermediate power levels between patients and healthy controls as illustrated in figure 2A-C. When comparing the power spectra of the three biotypes with HC, which can be seen in figure 2D-E, all biotypes demonstrate distinct patterns, though they generally follow the mean spectrum observed in patients. Biotype 2 and 3 shows the pronounced deviations from healthy controls, with a significant increase in power across all bands. This suggests a broad and substantial alteration in the EEG spectrum for Biotype 2 and 3, indicating potentially severe neurophysiological impact. In contrast, Biotype 1 demonstrates a different pattern, with significant decreases in Beta power, indicating a distinct form of EEG abnormality compared to the other biotypes.

These significances were identified by statistical analysis using ANOVA and Tukey's HSD and visualized via boxplots with scattered data points of each frequency band in the HC and biotypes groups as shown in figure 3A. The statistical comparison in figure 3B and 3C reveal that data under EO condition have almost the same significance as combined conditions, while data under EC condition shows much less significance. It is notable that EO is different from the combined conditions in the Gamma band, where Biotype 2 is no longer significant higher, however Biotype 1

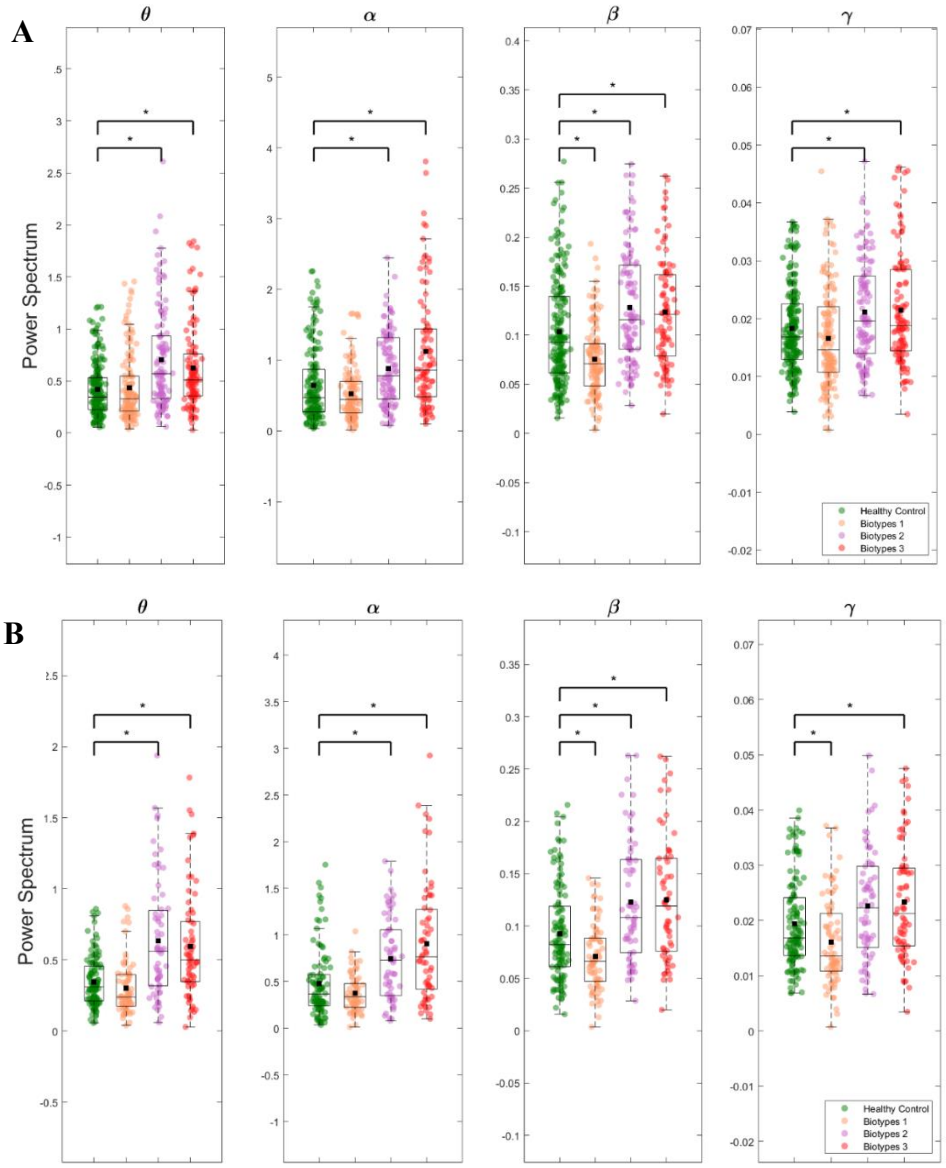

shows significantly lower power.

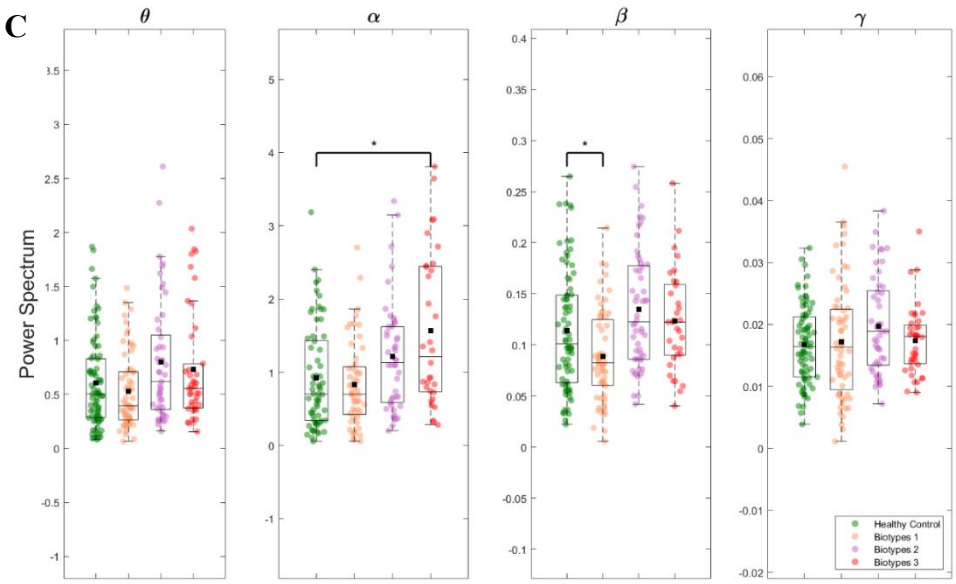

Figure 3: The figure illustrates the power spectrum comparison across four frequency bands (Theta, Alpha, Beta, and Gamma) between Healthy Controls and three Biotypes. (A) Combine EO and EC **(B)** EO, **(C)** EC. Within each frequency band, the dot represents individual subject data averaged over frequencies in that band, with boxplots displaying the median, mean (black dot) and the interquartile range. Significant differences are computed by ANOVA and Tukey's HSD and marked by asterisks (* $p<0.05$).

Sensor-Level Analysis

The sensor-level analysis used original EEG data to generate topographical plots (topoplots), offering a spatial visualization of EEG signal distribution across the scalp in different participant groups. These topoplots were first created for each group under EO condition to establish a foundational understanding of how EEG signals were distributed across the sensors and to identify potential group-specific differences in EEG activity.

To find out the distribution of group effects, statistical comparisons were conducted using t-tests on data from each channel. These t-tests aimed to statistically compare the EEG signals between different groups, and the results were visualized using difference topoplots. In these plots, EEG data from the HC group were subtracted from those of the patients' groups (including all patients and each of the three biotypes), highlighting the specific sensors or channels where EEG activity varied most significantly between groups.

As shown in the last column figure 4, when comparing the whole patients' group with the HC significant patterns primarily emerged in the Theta and Gamma bands. Initially, when applying a t-test, widespread significance ($p<0.5$) was observed across

the scalp in the Theta band, while in the Gamma band, significant differences were predominantly localized to the occipital region. In order to find in detail where the Theta power differs the most, A stricter criterion ($p<0.01$) was used in when applying the t tests. In this case, significant channels were found mainly in the frontal and parietal regions.

When examining the differences between the three biotypes and the HC group, as shown in the first three columns in Figure 4, it was evident that Biotype 2 and Biotype 3 showed patterns similar to those observed in patients, characterized by higher Theta and Gamma power in the same regions. Biotype 2, in particular, displayed a significant increase in the Theta band, which was more widespread compared to Biotype 3. In contrast, Biotype 1 showed much less difference across Theta and Gamma bands. The only significant decreased power was observed in beta band.

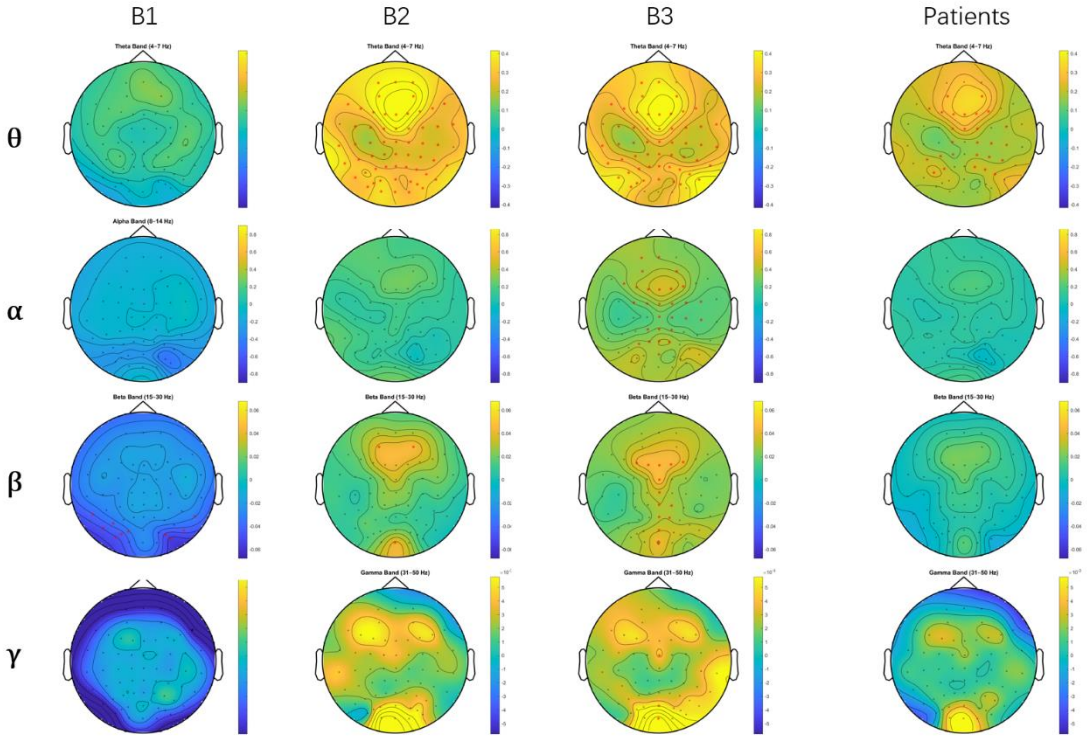

Figure 4: Topographical Maps of EEG Power Differences. This figure illustrates the differences in EEG power between HC and the patients' groups, including the three Biotypes and all patients, across the four frequencies bands, each column represents a different group (B1, B2, B3, Patients), and each row represents a specific frequency band. Warmer colors (yellow to red) indicate increased power in the Patients groups compared to HC, while cooler colors (green to blue) represent decreased power. Significant differences are computed by t test and marked by red asterisks (* $p<0.05$).

Source Reconstruction

In the source reconstruction analysis, the initial approach involved using

beamforming without any specific priors; however, this method did not yield clear target patterns. Consequently, the analysis shifted to using MSP with carefully selected anatomical priors derived from two key studies as mentioned in the methods section. These two sets of priors were applied in the context of the Theta (Figure 5) and Gamma (Figure 6) frequency bands, as well as across the full frequency range (Figure 7). The source reconstruction results were then compared to determine which priors are the best. The Symmonds priors has a higher percentage of variance explained (93.18% vs. 92.24%) and slightly better model fit which is showed by a less negative log-evidence value.

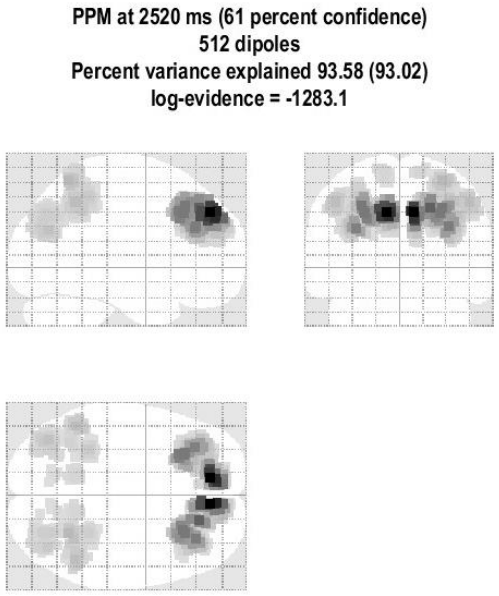

Figure 5: Theta Band Source Reconstruction Using Symmonds Priors. The plot shows the estimated neural response in the Theta band (4-8 Hz) using MSP with MNI coordinates (-29, -68, 49) and (29, -68, 49), and the left and right prefrontal cortices at MNI coordinates (-33, 45, 28) and (33, 45, 28) as priors. The reconstruction is based on the group mean data from HC. A strong fit was proved by the high percent variance explained (93.58%), with a log-evidence value of -1283.1.

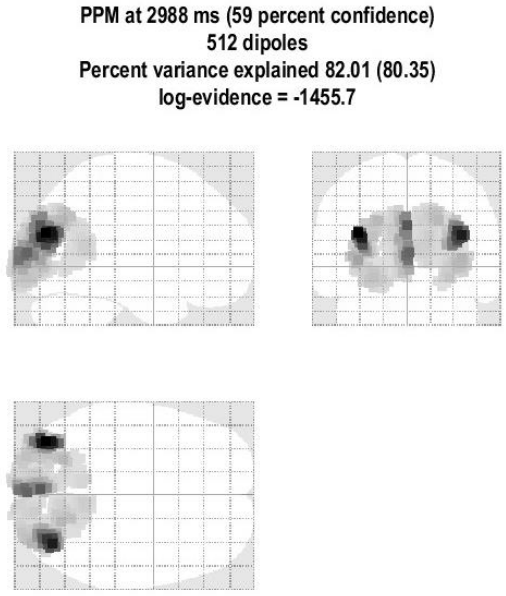

Figure 6: Gamma Band Source Reconstruction Using Tineke Grent-'t-Jong Priors. The plot shows the estimated neural response in the Gamma band (30-50 Hz) using MSP with MNI coordinates at [-11 -81 7] and [11 -78 9] as priors. The reconstruction also used grand mean data from the healthy control group. The percent variance explained is 82.01%, with a log-evidence value of -1455.7, suggesting a less robust fit compared to the Theta band reconstruction.

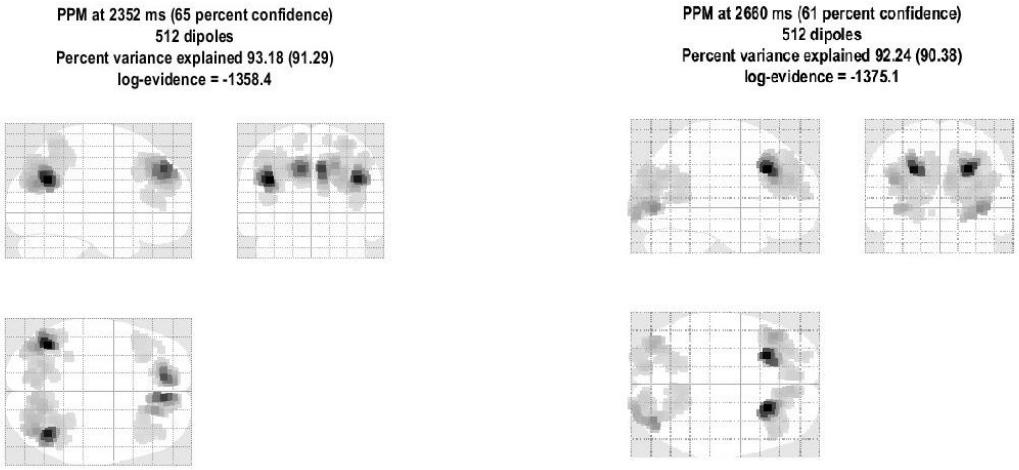

Figure 7: Symmonds vs. Combined Priors across the Full Frequency Bands. This figure compares the source reconstruction results using the Symmonds priors (left panel) and a combination of Symmonds and Tineke Grent-'t-Jong derived priors (right panel) across the full frequency range (4-50 Hz).

DCM Analysis

DCMs were conducted using both individual subject data and group grand mean

data, targeting the effective connectivity across regions defined by the chosen coordinates in the Theta and Gamma frequency bands. Unfortunately, all DCMs failed to provide a satisfactory fit to the data. This outcome suggested that the applied CMC models (spm_fx_cmc_ei_v1), even less restrictions (spm_fx_cmc_2017_constG), did not capture the neural processes underlying the EEG data in this study.

Following the failure of the initial DCMs to produce adequate fits, simulations were conducted to investigate how parameter adjustments could better approximate the empirical data. This process also used the same two models, However, the simulations using spm_fx_cmc_ei_v1 failed to produce realistic EEG patterns, particularly in replicating the alpha peak observed in healthy controls. The approach was then revised by adopting (spm_fx_cmc_2017_constG).

In this model, systematic tuning of specific parameters proved crucial for generating the desired spectral characteristics. The third synaptic time constant (T(3)) was increased from 16 to 39 ms, which slowed synaptic responses. The slope of the activation function (S) was decreased from 1 to 0.7, making neurons less responsive to input signals. This adjustment modulated the firing rates, contributing to the emergence of an alpha peak in the simulated data. Each of the 12 intrinsic connectivity parameters was then systematically altered within a range of 30% to examine their effects on replicating the observed differences between the three biotypes and healthy controls (HC).

The alternation of each of the 12 intrinsic connections revealed distinct patterns that could be corresponded with the different biotypes. Four specific connections were found to able to reproduce part of the biotypes' spectra patterns as illustrated by Figure 8. First, reducing the self-inhibition among inhibitory interneurons (ii-ii) was found to reproduce the EEG patterns associated with Biotype 2 and 3, including increased Theta and Alpha power. The ii-ii connection represents the self-regulatory mechanism within inhibitory interneurons, and its reduction leads to a loss of inhibitory control, potentially causing a widespread imbalance between excitation and inhibition (E/I) across the cortex. Similarly, the reduction in the excitatory input from Spiny Stellate cells to superficial pyramidal cells (ss-sp) was linked to Biotype 2 and 3 with increased theta power. For Biotype 1, both reduced excitatory input from Spiny Stellate cells to inhibitory interneurons (ss-ii) and reduced inhibitory feedback from interneurons to superficial pyramidal cells (ii-sp) was able to replicate the reduced alpha peak.

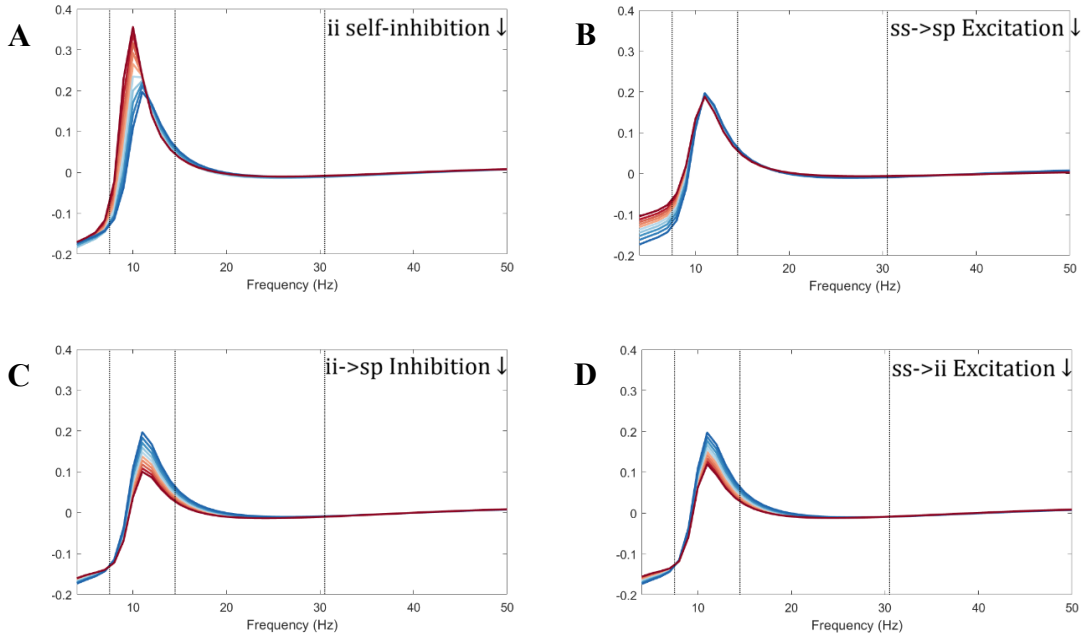

Figure 8: Impact of altering specific intrinsic connections on EEG power spectra across mainly Theta and Alpha bands. (A) Reduced self-inhibition among inhibitory interneurons (ii→ii). **(B)** Reduced excitation from spiny stellate cells to superficial pyramidal cells (ss→sp). **(C)** Reduced inhibition from inhibitory interneurons to superficial pyramidal cells (ii→sp). **(D)** Reduced excitation from spiny stellate cells to inhibitory interneurons (ss→ii). Each simulation transitions from control (Con, dark blue) to more extreme psychotic conditions (Scz, dark red).

Discussion

The initial analysis of PSD and sensor-level topographic results revealed significant differences in the theta and gamma bands between patients with psychosis and healthy controls. Specifically, for biotypes 2 and 3, differences in the theta band were associated with the default mode network, which includes the frontal and parietal regions. Gamma band differences, on the other hand, were correlated to the occipital regions. These findings are aligned with previous literatures[4, 12, 13]. The most pronounced deviations were observed in biotype 3, which exhibited substantial increases in both theta and gamma power, indicating a severe neurophysiological disruption. Biotype 2 showed similar but less severe alterations, particularly in the theta band. However, biotype 1 demonstrated a unique pattern characterized by decreased beta power, suggesting a different underlying neurobiological mechanism compared to the other biotypes. These early results suggest that biotype-specific spectral power differences reflect distinct connectivity alterations, which could provide insight into the diverse neurobiological profiles of psychosis.

This study has revealed the possible changes of the intrinsic connection parameters that may be responsible for the different EEG patterns seen in different psychosis biotypes. Decreased self-inhibition of inhibitory interneurons (ii-ii) and decreased excitatory inputs from spiny stellate cells to inhibitory interneurons (ss-ii) were seen to mimic the EEG changes of specific biotypes. These results suggest that the biotype-specific features may result from particular dysfunctions in the excitatory/inhibitory balance of the cortex, which are expressed in the changes in the connectivity. These findings indicate that psychotic symptoms may originate from specific disruptions in the cortical excitatory/inhibitory balance, which are reflected in the altered connectivity patterns.

Of interest is the difference between the results of the present study and those of Clementz et al. (2016) who endorsed the three psychosis dimensions. In their study, they stated that biotype 2 had the highest resting state EEG power associated with sensorimotor reactivity. However, this finding does not match with my PSD findings, in which biotype 2 did not have the highest intrinsic neural activity compared with all other groups. One possible reason for this inconsistency might be due to a possibility that Clementz et al. (2016) have focused on a narrower or different range of frequency that were particularly correlated to sensorimotor reactivity, whereas this analysis covered a more comprehensive range of frequencies and therefore might not have revealed frequency specific effects.

Several challenges and limitations were noticed in this study. One major limitation was that only one model structure was employed, and this model structure might not have been versatile enough to reproduce the diverse features of the neural activity in different frequency bands. the canonical microcircuit model itself or even with the priors used in the simulation could not well fit the EEG data. Also, the simulation results could not produce clear patterns in the beta and gamma bands, that are crucial for elucidating the dysconnectivity of the cortex in psychosis, is also a challenge that need to be overcome. The results suggest that other forms of models with different structures can be beneficial in describing the data if they are equipped with biologically realistic priors. This limitation suggests that there is a need to fine-tune some of the model parameters such as employing better priors that are specific to the neurobiology of psychosis.

The third major problem concerns with the methods employed for the treatment of outliers. The outliers were managed in two ways in this study; either the entire subjects were excluded or only certain channel-frequency data points. Nevertheless, such various strategies of outlier elimination could result in the different results and affect the group EEG patterns identified. The values at which outliers are identified is also

another important factor which affects the results and if these thresholds are changed then different group effects can be observed. Also, the absence of longitudinal data in this study limits the understanding of the effects of disease progression or aging on connectivity, which could help elucidate the patterns of connectivity alterations over time.

Further research should be directed towards the improvement of the models employed in this research. One critical direction for enhancement is the incorporation of biologically more plausible priors, which may be obtained from more diverse studies. More advanced techniques for tuning the parameters might be employed to update these priors to keep them within biological reasonable ranges as well as enhancing the quality of the model fitting. It would also be helpful to consider longitudinal information in further studies, since it might be possible to observe changes of EEG patterns during time or disease course. This approach might give more information on the temporal dimension of the neural dysregulation which occurs in psychosis.

In conclusion, the current study reveals the important changes in synaptic functioning that may contribute to the different EEG profiles in various psychosis biotypes. In particular, the reduced self-inhibition detected in inhibitory interneurons (ii-ii) and the decrease in the excitatory connections from spiny stellate cells to inhibitory interneurons (ss-ii) were shown to mimic the EEG changes characteristic of certain biotypes. These results suggest that psychotic symptoms may result from reduced synaptic gain or certain dysregulation of cortical excitatory-inhibitory processes, which are expressed in the changes in connectivity. These findings can be useful for future work to further improve neural models and for the clarification of the nature of psychosis.

ACADEMIC ACKNOWLEDGEMENT

I am deeply grateful to Dr. Rick Adams and Julia Rodriguez Sanchez for their exceptional guidance and expertise, which played a pivotal role in shaping both the design and analysis of my project. Their thoughtful insights were crucial to the success of this research. I would also like to acknowledge Amruth Sagar Gadey for kindly providing him simulation method, which became a vital tool for this study. The collective support and contributions of all three have been fundamental to the completion of this research effort.

References

1. Association AP. Diagnostic and statistical manual of mental disorders. 5th ed. Arlington, Va: American Psychiatric Association; 2013.
2. Keshavan MS, Morris DW, Sweeney JA, Pearlson G, Thaker G, Seidman LJ, et al. A dimensional approach to the psychosis spectrum between bipolar disorder and schizophrenia: the Schizo-Bipolar Scale. Schizophr Res. 2011;133(1-3):250-4.
3. Meyer-Lindenberg A. From maps to mechanisms through neuroimaging of schizophrenia. Nature (London). 2010;468(7321):194-202.
4. Adams RA, Pinotsis D, Tsirlis K, Unruh L, Mahajan A, Horas AM, et al. Computational Modeling of Electroencephalography and Functional Magnetic Resonance Imaging Paradigms Indicates a Consistent Loss of Pyramidal Cell Synaptic Gain in Schizophrenia. Biol Psychiatry. 2022;91(2):202-15.
5. Friston KJ, Harrison L, Penny W. Dynamic causal modelling. NeuroImage (Orlando, Fla). 2003;19(4):1273-302.
6. Clementz BA, Sweeney JA, Hamm JP, Ivleva EI, Ethridge LE, Pearlson GD, et al. Identification of Distinct Psychosis Biotypes Using Brain-Based Biomarkers. Am J Psychiatry. 2016;173(4):373-84.
7. Welch P. The use of fast Fourier transform for the estimation of power spectra: A method based on time averaging over short, modified periodograms. IEEE transactions on audio and electroacoustics. 1967;15(2):70-3.
8. Moran R, Pinotsis DA, Friston K. Neural masses and fields in dynamic causal modeling. Front Comput Neurosci. 2013;7:57.
9. Hampel FR. Robust statistics : the approach based on influence functions / Frank R. Hampel ... [et al.]. New York ;: Wiley; 1986.
10. Oostenveld R, Fries P, Maris E, Schoffelen JM. FieldTrip: Open source software for advanced analysis of MEG, EEG, and invasive electrophysiological data. Comput Intell Neurosci. 2011;2011:156869.
11. Friston K, Harrison L, Daunizeau J, Kiebel S, Phillips C, Trujillo-Barreto N, et al. Multiple sparse priors for the M/EEG inverse problem. Neuroimage. 2008;39(3):1104-20.
12. Symmonds M, Moran CH, Leite MI, Buckley C, Irani SR, Stephan KE, et al. Ion channels in EEG: isolating channel dysfunction in NMDA receptor antibody encephalitis. 2018.
13. Grent-'t-Jong T, Gross J, Goense J, Wibral M, Gajwani R, Gumley AI, et al. Resting-state gamma-band power alterations in schizophrenia reveal E/I-balance abnormalities across illness-stages. eLife. 2018;7:e37799.
14. Lacadie CM, Fulbright RK, Rajeevan N, Constable RT, Papademetris X. More accurate Talairach coordinates for neuroimaging using non-linear registration. Neuroimage. 2008;42(2):717-25.